Influence de la rugosité de surface sur les champs mécaniques locaux dans les agrégats polycristallins

Yoann Guilhem, Stéphanie Basseville, Henry Proudhon, Georges Cailletaud

Influence de la rugosité de surface sur les champs mécaniques locaux dans les agrégats polycristallins

Influence of surface roughness on local mechanical fields in polycrystalline aggregates

Y. Guilhem[a], S. Basseville[b], H. Proudhon[c], G. Cailletaud[c]

a. *MATEIS, INSA de Lyon, CNRS UMR 5510*
b. *LISV, Université de Versailles Saint-Quentin, 45 avenue des Etats-Unis, 78000 Versailles, France*
c. *MINES ParisTech, Centre des Matériaux, CNRS UMR 7633, BP 87, 91003 Evry Cedex, France*

Résumé :

Cet article est dédié à l'étude de l'influence de la rugosité de surface, générée par les processus d'élaboration industriels, sur les champs locaux dans les agrégats polycristallins. L'étude se concentre sur l'effet des singularités géométriques seules. Des calculs Éléments Finis sont effectués avec un modèle de plasticité cristalline sur un agrégat polycristallin d'acier inoxydable 316L comportant différents états de rugosité en surface. Une analyse est conduite sur la dépendance des champs déformation plastique locale vis-à-vis de l'état de surface. Elle montre que la rugosité de surface peut changer drastiquement les schémas de localisation induits par la cristallographie. Néanmoins, la portée de cet effet se limite généralement à la première couche de grains en surface. Une règle simple est proposée pour définir la profondeur de la zone affectée en fonction du niveau de rugosité.

Abstract :

This paper is dedicated to the study of the influence of surface roughness, due to industrial processes, on the local fields inside polycrystals. It is focused on the effect of geometrical singularities. Finite element computations are performed with a crystal plasticity model on a 316L stainless steel polycrystalline aggregate with different roughness states at the free surface. The analysis is conducted on the plastic strain localization patterns depending on the surface state. This study shows that surface roughness can strongly modify the plastic strain localization caused by crystallography. Nevertheless, this effect takes places mainly at the surface and vanishes under the first layer of grains. A simple rule is proposed to define the depth of the affected zone depending on the roughness level.

Mots clefs : **polycrystal, roughness, localization**

1 Introduction

Fatigue life prediction is studied for several decades because of the variety of parameters which can define the conditions of a fatigue test. In the case of short fatigue cracks, the microstructural features, such as grain boundaries, play a very important role in the early stages of crack growth. Nowadays, researchers are investigating the role of local microstructure in the evolution of short fatigue cracks in Titanium polycrystals [1]. Initiation is usually due to plastic strain localization in persistent slip bands at the surface, generated by crystallographic slip. However the macroscopic features, e.g. surface roughness, should not be neglected because there are interactions and competitions between the different phenomena observed at each scale. LCF fatigue tests on 304L steel specimen with different surface roughness carried out under vacuum showed that increasing the Root Mean Square (RMS) by a factor of ten halved the fatigue crack initiation period [2].

In order to study the competition of the rough surface effect with crystallographic damage mechanisms, numerical simulations provide a useful tool to explore all kinds of parameters. The improvements in experimental techniques allow now to perform simulations on real 3D microstructures and to compare the results with strain field measurements. A previous study made on 304L steel, with real microstructure from EBSD mapping, considering surface roughness and local pre-hardening showed that these two parameters have respectively negative and positive effects on fatigue life [3]. In this study we proposed to investigate the role of surface roughness apart from all other surface state parameters and its competition with microstructural strain mechanisms. To achieve this tasks Finite Element Computations of polycrystalline aggregates with crystal plasticity model are performed, followed by the analysis of plastic strain localization at the surface, inside the volume and from a statistical point of view.

2 Numerical model

2.1 Crystal plasticity

The Méric–Cailletaud crystal plasticity model is introduced in the finite element suite Z-set [4]. Small strain assumption is used, which seems reasonable, since, in our past experience, the amount of rotation of a slip plane is around 1° for 1% macroscopic strain. Each grain is considered as a single crystal and the displacement fields are supposed to be continuous at grain boundaries. Strain rate tensor is composed of an elastic and a viscoplastic part:

$$\dot{\underset{\sim}{\boldsymbol{\varepsilon}}} = \dot{\underset{\sim}{\boldsymbol{\varepsilon}}}^e + \dot{\underset{\sim}{\boldsymbol{\varepsilon}}}^p = \underset{\approx}{\boldsymbol{C}}^{-1} : \dot{\underset{\sim}{\boldsymbol{\sigma}}} + \dot{\underset{\sim}{\boldsymbol{\varepsilon}}}^p \tag{1}$$

Cubic elasticity is defined by the fourth order tensor of elastic moduli $\underset{\approx}{\boldsymbol{C}}$. Hence elasticity itself produces residual intergranular stresses.

The resolved shear stress τ^s is computed on slip system s by means of the orientation tensor $\underset{\sim}{\boldsymbol{m}}^s$:

$$\tau^s = \underset{\sim}{\boldsymbol{\sigma}} : \underset{\sim}{\boldsymbol{m}}^s \tag{2}$$

$$\text{with } \underset{\sim}{\boldsymbol{m}}^s = \frac{1}{2}\left(\underline{\boldsymbol{l}}^s \otimes \underline{\boldsymbol{n}}^s + \underline{\boldsymbol{n}}^s \otimes \underline{\boldsymbol{l}}^s\right) \tag{3}$$

where $\underline{\boldsymbol{n}}^s$ is the normal to the slip plane and $\underline{\boldsymbol{l}}^s$ is the slip direction.

The viscoplastic strain rate tensor is defined as the sum of the contributions of all the slip systems s. Each viscoplastic slip rate $\dot{\gamma}^s$ is given by a Norton law, function of the resolved shear stress, the critical resolved shear stress τ_0 and two variables ; x^s for kinematic hardening and r^s for isotropic hardening.

$$\dot{\underset{\sim}{\boldsymbol{\varepsilon}}}^p = \sum_s \dot{\gamma}^s \underset{\sim}{\boldsymbol{m}}^s \tag{4}$$

$$\dot{\gamma}^s = \text{sign}(\tau^s - x^s)\dot{v}^s \tag{5}$$

$$\dot{v}^s = \left\langle \frac{|\tau^s - x^s| - r^s - \tau_0}{K} \right\rangle^n \tag{6}$$

where K and n are the parameters which define viscosity, $\dot{v}^s$ stands for slip rate, v^s is the cumulated viscoplastic slip on slip system s.

Hardening depends on two internal state variables, α^s for kinematic and ρ^s for isotropic hardening, as described by equations 7 to 10.

$$x^s = c\alpha^s \tag{7}$$

$$r^s = bQ \sum_r h_{sr}\rho^r \tag{8}$$

$$\dot{\alpha}^s = \left(\text{sign}(\tau^s - x^s) - d\alpha^s\right)\dot{v}^s \tag{9}$$

$$\dot{\rho}^s = (1 - b\rho^s)\dot{v}^s \tag{10}$$

where c and d are material parameters for kinematic hardening, Q and b are material parameters for isotropic hardening. Self-hardening and latent hardening between different slip systems are characterized by the interaction matrix components h_{sr}. The material of the study is an austenitic stainless steel, the crystallographic structure of which is FCC, and where slip operates on octahedral slip systems, which are defined by slip plane normal family $\{1\ 1\ 1\}$ and slip direction family $\langle 1\ 1\ 0 \rangle$. The corresponding interaction matrix is defined by six coefficient h_i [5].

2.2 Mesh and boundary conditions

The polycrystalline aggregate reference mesh used here is built by Voronoi tessellation as explained in a previous study [6]. A rough surface is generated from onedimensionnal roughness profile measured on a brushed surface state component, which mainly consists in streaks (see figure 1c). This profile is then extended along x axis (see figure 1d) and Brownian noise is added on the resulting surface to provide the final synthetic rough surface (see figure 1e). To apply this rough surface on the mesh, the node displacement method has been chosen, not only on the surface but also on bulk nodes to avoid degenerated elements. Until a depth of 62.5 µm below the free surface Z_1 (where the displacement become nil), the nodes displacement is linearly linked to the distance to the free surface (where the displacement is equal to the rough surface).

To study the effect of the roughness intensity, different rough meshes are generated by multiplying the roughness values by a factor r between 0 and 1. For instance, for $r = 0.5$, only the half of the roughness displacement is applied and the mesh is named `brushed_0.5`.

The boundary conditions basically consist in symmetry boundary conditions over all hidden faces (X_0 Y_0 and Z_0), free surface condition on face Z_1, and a uniaxial cyclic loading in y direction (see figure 1a). In more details, the conditions applied on each face are the following:

- $u_x = 0$ on face X_0
- $u_y = 0$ on face Y_0
- $u_z = 0$ on face Z_0
- u_x homogeneous, set by MPC on face X_1
- u_y homogeneous, resulting in $\varepsilon_{yy} = \pm 0.2\%$ on face Y_1
- $\sigma_{zz} = 0$ on face Z_1

3 Results and discussion

3.1 Surface analysis

The sum of accumulated plastic slip over all slip systems $\sum \gamma_{cum}$, is considered as the plastic strain variable. A selection of the results is shown in figure 2, where the plastic strain contour maps at the free surface Z_1 can be compared to the roughness contour maps. First, we compare flat (figure 2e) and brushed_1.0 cases (figure 2h). The localization band patterns, oriented at 45° with respect to the loading direction, classically observed on flat aggregates are modified in presence of roughness. Well-oriented grains, grain boundaries and triple point localization is mainly replaced by relief valleys localization, which means a real decrease in the crystallographic influence on plastic strain localization. However, some discontinuities still appear at some grain boundaries, even at the bottom of the valleys. Then, with a gradual roughness intensity, from case brushed_0.2 to brushed_1.0 (figures 2f to 2h), a progressive transition between the two types of localization is exhibited. At first sight, the brushed_0.2 case is almost the same as the flat case, but some differences are noticeable – at triple points for instance.

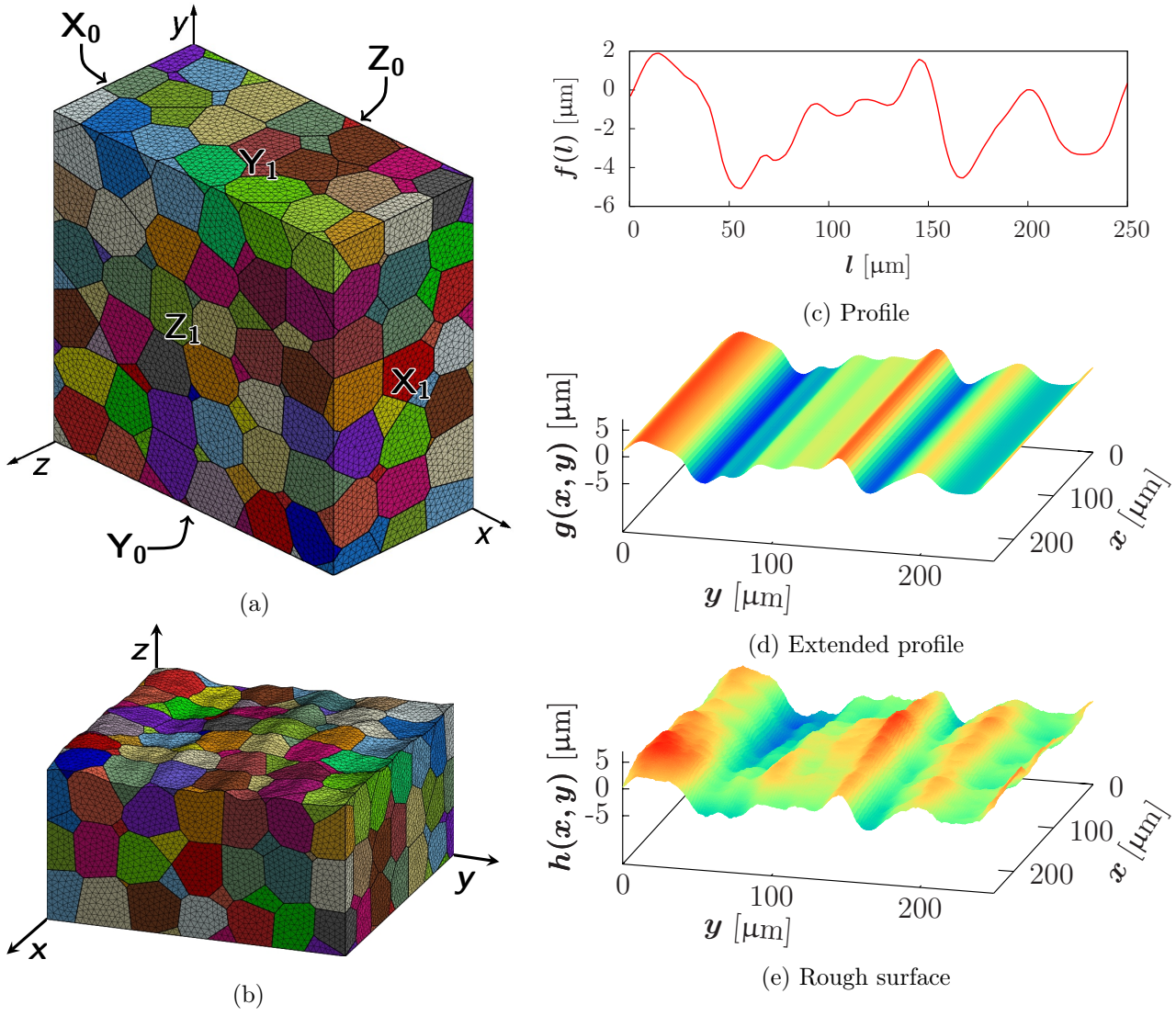

Figure 1: (a) Polycrystalline aggregate mesh with face definition for the boundary conditions. (b) Rough mesh surface brushing. (c) Roughness profile for brushed state [3], (d) profile extension and (e) final mesh surface

3.2 Volume analysis

Investigating plastic strain map at the surface is not enough, especially because fatigue crack growth is a 3D problem and depends a lot on the microstructure below the surface. Figure 3 reveals plastic strain slice snapshots in the xz plane of the flat and brushed_1.0 cases. Again, we can clearly distinguish the zones affected by the surface relief. But when inspecting zones beyond the first layer of grains below the surface, the differences between flat and rough cases vanish. This demonstrates that the effect of surface roughness remains limited to a certain depth which has to be defined, depending on the surface state.

3.3 Statistical analysis

To quantify the depth of the affected zone, we provide a statistical analysis based on the plastic strain distribution for a wider range of roughness intensity (0.1, 0.2, 0.3, 0.5 and 1.0). We are using the ratio between the variable obtained in the rough case to the reference case (flat aggregate), defined as $R(\sum \gamma_{cum}) = \frac{\sum \gamma_{cum}(rough)}{\sum \gamma_{cum}(flat)}$. This ratio is plotted for each integration point of each surface state in figure 4a. The distance to the line $R = 1$ highlight the effect of roughness. Figure 4b shows the

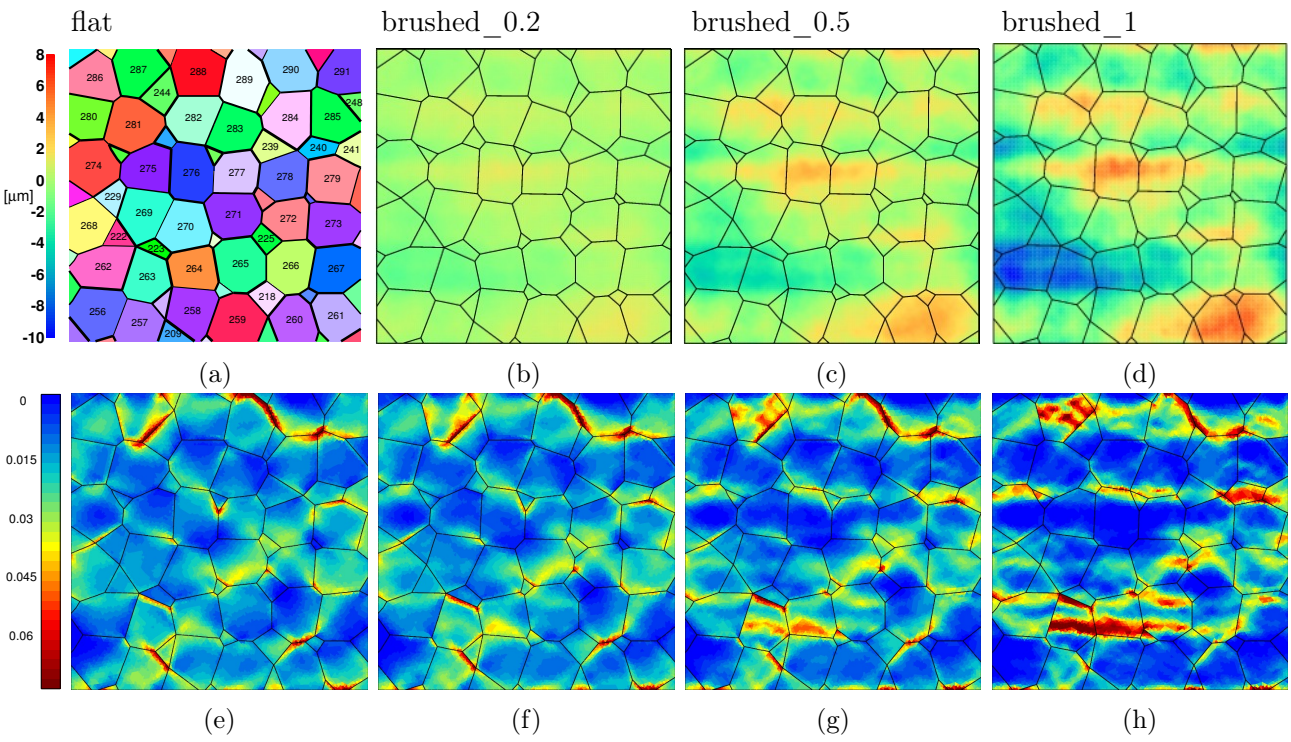

Figure 2: (a) EBSD mapping of the free surface. (b) to (e) Relief map for each rough case. (f) to (j) Plastic strain $\sum \gamma_{cum}$ contour surface map.

evolution of the standard deviation depending on the distance to the free surface The critical distance d_{crit} is defined by the distance to the free surface where the standard deviation of the ratio $R(\sum \gamma_{cum})$ is less than 0.1. That means that approximately 99.7% of the values at this depth are affected by a ratio lower than 5.0×10^{-3} in the case of a Gaussian distribution. One can measure the correlation between the RMS of the rough surface and the determined critical distance in figure 4c. The evolution is linear with a slight offset, so that the surface roughness could be neglected when the RMS of a brushed surface is less than about 0.25 µm.

4 Conclusions

In this paper, we used Finite Element crystal plasticity to highlight the effect of surface roughness on the plastic strain localization at the surface of polycrystals. We noticed a drastic change in the localization patterns when comparing the results on flat and brushed surfaces, where the plastic strain tends to localize at the bottom of the relief valleys. In terms of plastic strain localization, there is a clear competition between the local crystalline orientation and the surface relief. Nevertheless, a volumetric analysis showed that this effect seems to be limited to the first layer of grain below the surface. To give a quantitative relation between the roughness and the critical zone influenced by a brushed surface, many computations with gradual RMS were carried on, followed by a statistical analysis. The results showed that the thickness of this layer below the surface is linearly correlated to the surface RMS by a factor of 16.

This study is based on a model which remains too simple because the others parameters like residual stresses or hardening were not introduced. However, these conclusions show that polycrystalline aggregate computations should take into account surface roughness especially when they are focusing on the surface fields.

References

[1] M. Herbig, A. King, P. Reischig, H. Proudhon, E.M. Lauridsen, J. Marrow, J.-Y. Buffière, and W. Ludwig. 3-D growth of a short fatigue crack within a polycrystalline microstructure studied

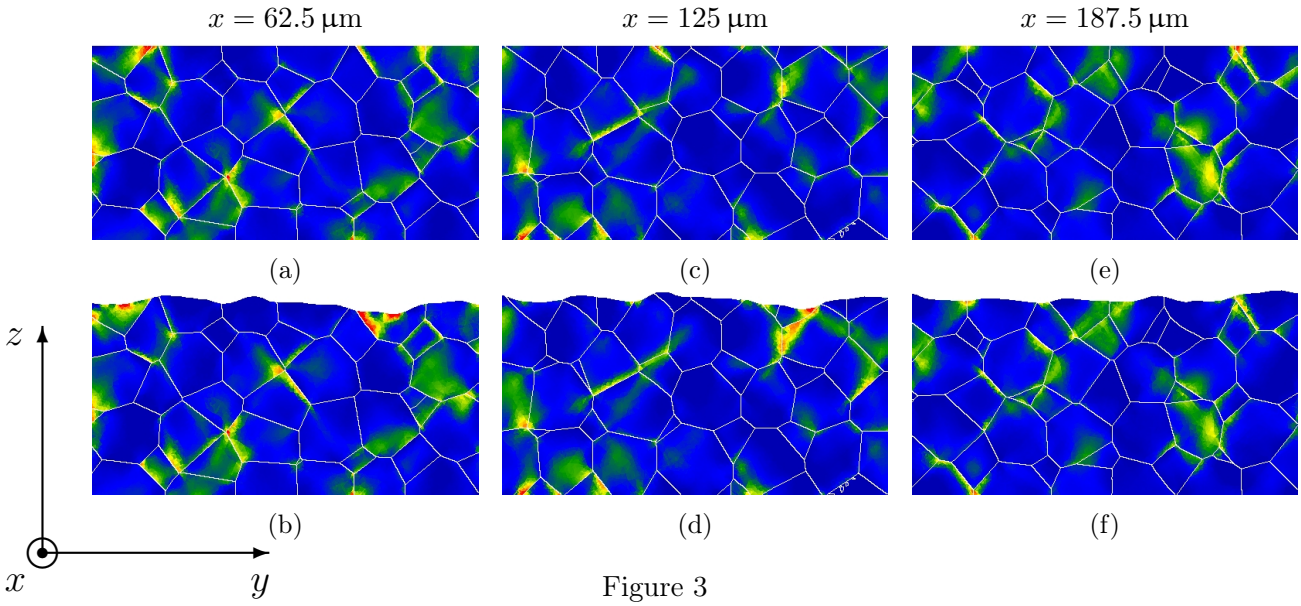

Figure 3

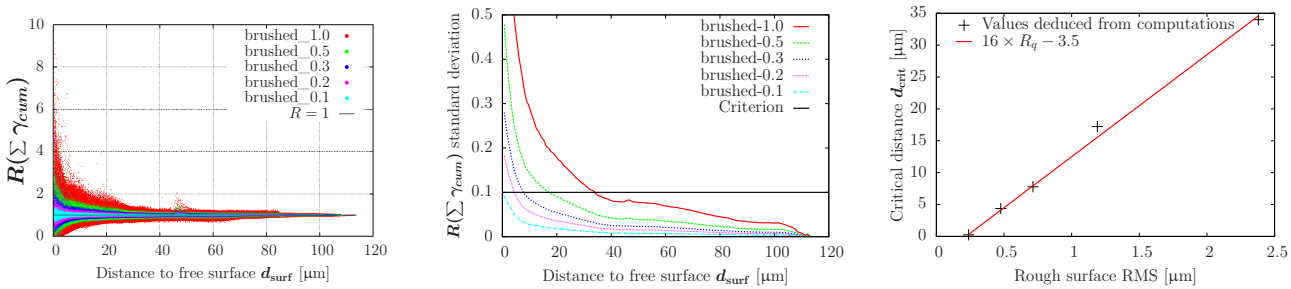

(a) (b) (c)

Figure 4: Statistical analysis of the distribution of plastic strain comparison ratio $R(\sum \gamma_{cum})$ for each surface state. (a) Gauss point values and (b) standard deviation of $R(\sum \gamma_{cum})$ versus distance to the free surface d_{surf}. (c) Critical distance d_{crit} versus surface RMS.

using combined diffraction and phase-contrast X-ray tomography. *Acta Mat.*, 59:590–601, 2011.

[2] J.M. Lee and S.W. Nam. Effect of crack initiation mode on low cycle fatigue life of type 304 stainless steel with surface roughness. *Material Letters*, 10(6):223–230, 1990.

[3] A. Le Pécheur, F. Curtit, M. Clavel, J.-M. Stéphan, C. Rey, and P Bompard. Polycrystal modelling of fatigue: Pre-hardening and surface roughness effects on damage initiation for 304L stainless steel. *Int. J. Fatigue*, 45:48–60, 2012.

[4] L. Méric and G. Cailletaud. Single crystal modeling for structural calculations. Part 2: Finite element implementation. *J. of Engng. Mat. Technol.*, 113:171–182, 1991.

[5] P. Franciosi. The concepts of latent hardening and strain hardening in metallic single crystals. *Acta Metall.*, 33:1601–1612, 1985.

[6] Y. Guilhem, S. Basseville, F. Curtit, J-M. Stéphan, and G. Cailletaud. Numerical investigations of the free surface effect in three-dimensional polycrystalline aggregates. *Computational Materials Science*, 70:150–162, 2013.